scientific reports

Check for updates

OPEN

Publisher Correction: Elucidating the relationship between affinity and potency in the performance of therapeutic IgE

Published online: 15 May 2026

Francesca Marano, Callum McKenzie, James R. Birtley, Sadaf A. Hussain, Olivia Macleod, Alexander Goodacre, Shuang Wu, Oliver E. Amin, Nikhil Faulkner, John Devlin, Liam Regan, Komal Soni, Rachel M. Johnson, Valerie E. Pye, Tim Wilson, Elizabeth Hardaker & Kevin FitzGerald

Correction to: *Scientific Reports* https://doi.org/10.1038/s41598-026-43772-6, published online 30 March 2026

The original version of this Article contained errors in Figures 1, 2, 3, and 4 where, due to processing error during production, certain elements of the Figures became illegible or elements were omitted entirely. In Figure 1, element 1A and 1D the red highlighted letters of the sequences drifted and overlapped with the rest of the amino acids making the Figure less legible. Additionally, graphical element of 1B is erroneously omitted. The original Figure 1 appears below.

In Figure 2 the graphical elements of 2B, 2E and 2F were erroneously omitted. The original Figure 2 appears below.

In Figure 3 all the graphical elements are erroneously omitted, and the blue, pink, green, and grey letters of the sequence overlap with the rest of amino acid sequences making the Figure less legible. The original Figure 3 appears below.

Lastly in Figure 4 the graphical element of 4I is erroneously omitted. The original Figure 4 appears below.

The original Article has been corrected.

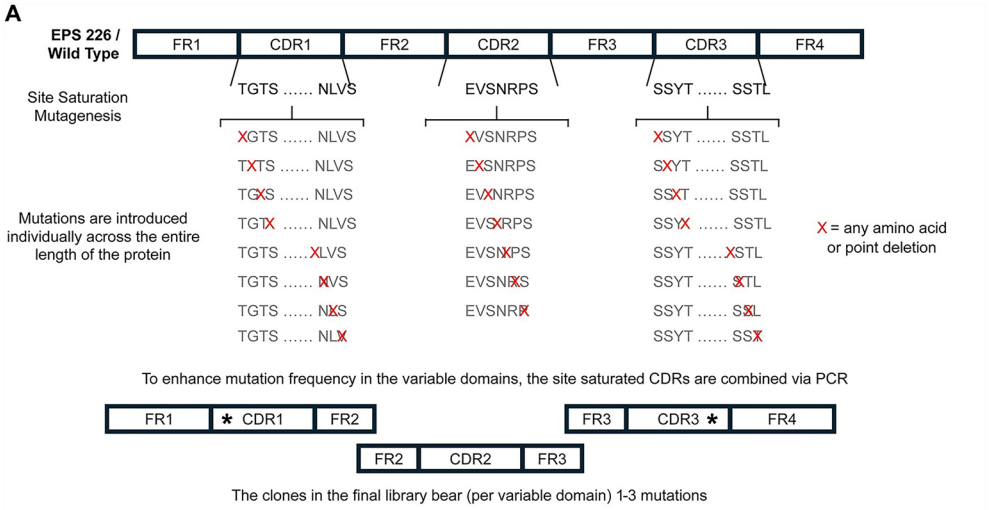

B

Clone n.	Alias	K_d human HER2 (M)	Potency EC50 (M)	K_d rat HER2 (M)
	EPS 226 / WT	2.67E-8	2.08E-10	2.09E-8
Clone 4		5.77E-9	6.40E-11	6.64E-9
Clone 5	EPS 232	2.87E-9	3.60E-11	1.98E-9
Clone 9		9.93E-10	5.20E-11	6.21E-10

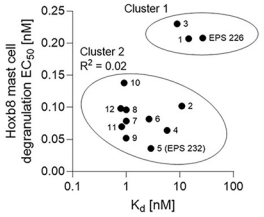

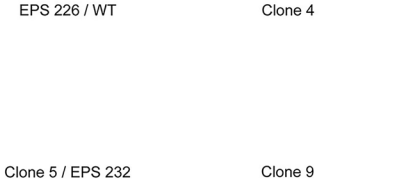

D

VH Family: IGHV1-3*01

Molecule	HCDR1	HCDR2	HCDR3
EPS 226 / WT	SYAMH	WINAGNGNTKYSQKFQG	DFSSQVATAAVDY
Clone 9	SYAMH	WINAGNGNTKYTKFQG	DFSSQVATAAVDY

VL Family: IGLV2-14*02

Molecule	LCDR1	LCDR2	LCDR3
EPS 226 / WT	TGTSSDVGSYNLVS	EVSNRPS	SSYTSSSTL
Clone 4	TGTSSDVGSYNLVS	TVSNRPS	SSYTSSSTL
Clone 5	TGTSSDVGSYNLVS	TVSNRPS	SSYTSSSL
Clone 9	TGTSSDVGSYNLVS	TVSNRPS	SSYT-SSTL

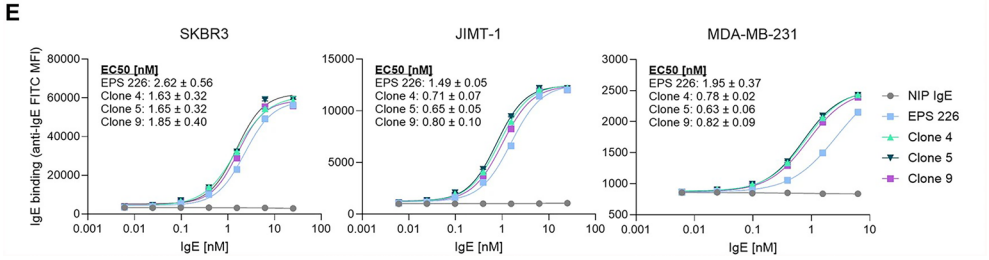

◀**Fig. 1**. Mutagenesis campaign identifies novel affinity-matured HER2-targeting IgE. (**A**) Mutagenesis strategy used to construct the Fab phage display library. A synthetic DNA library was designed such that each amino acid position within the CDRs was individually substituted with all other 19 amino acids (Site-Saturation Mutagenesis) or deleted. To enhance library diversity and enable the analysis of the effects of multiple simultaneous mutations on binding affinity, saturated CDR variants were assembled using conserved framework region homology. This strategy allows each clone in the library to carry between 1 and 3 mutations (random point mutations in the CDRs are indicated with *) in each of the heavy and light chain domains. The resulting DNA library was electroporated into *E. coli* TG1 cells and phage display selection was performed by panning against decreasing concentrations of human HER2. (**B**) Top: Binding affinity and mast cell degranulation potency measurements of the parental and affinity matured Fab and full length IgE clones, respectively. Binding affinities were determined using BLI. Kd values were measured against both human and rat HER2. Reported values represent the average of three independent measurements for each antigen. Hoxb8 EC50 values are from Supplementary Figure 1A. Bottom: Representative BLI sensorgrams for the parental Fab and affinity matured Fab clones 4, 5 (EPS 232) and 9 bound to human HER2. (**C**) Hoxb8 mast cell degranulation EC50 versus the monovalent human HER2 affinity. R2, coefficient of determination. Values are from Supplementary Fig. 1A. (**D**) Amino acid sequence of the heavy and light CDRs of EPS 226 and clones 4, 5 (EPS 232) and 9, with their respective modifications highlighted in red. (**E**) SKBR3, JIMT-1, and MDA-MB-231 cells were treated with either full length NIP IgE, EPS 226, or clones 4, 5, or 9; where bound IgE was detected using an anti-IgE FITC conjugated antibody. Data points show mean average, error bars are standard error of the mean (SEM), n = 6, three independent experiments, MFI—median fluorescence intensity, mean EC50 value shown ± SEM.

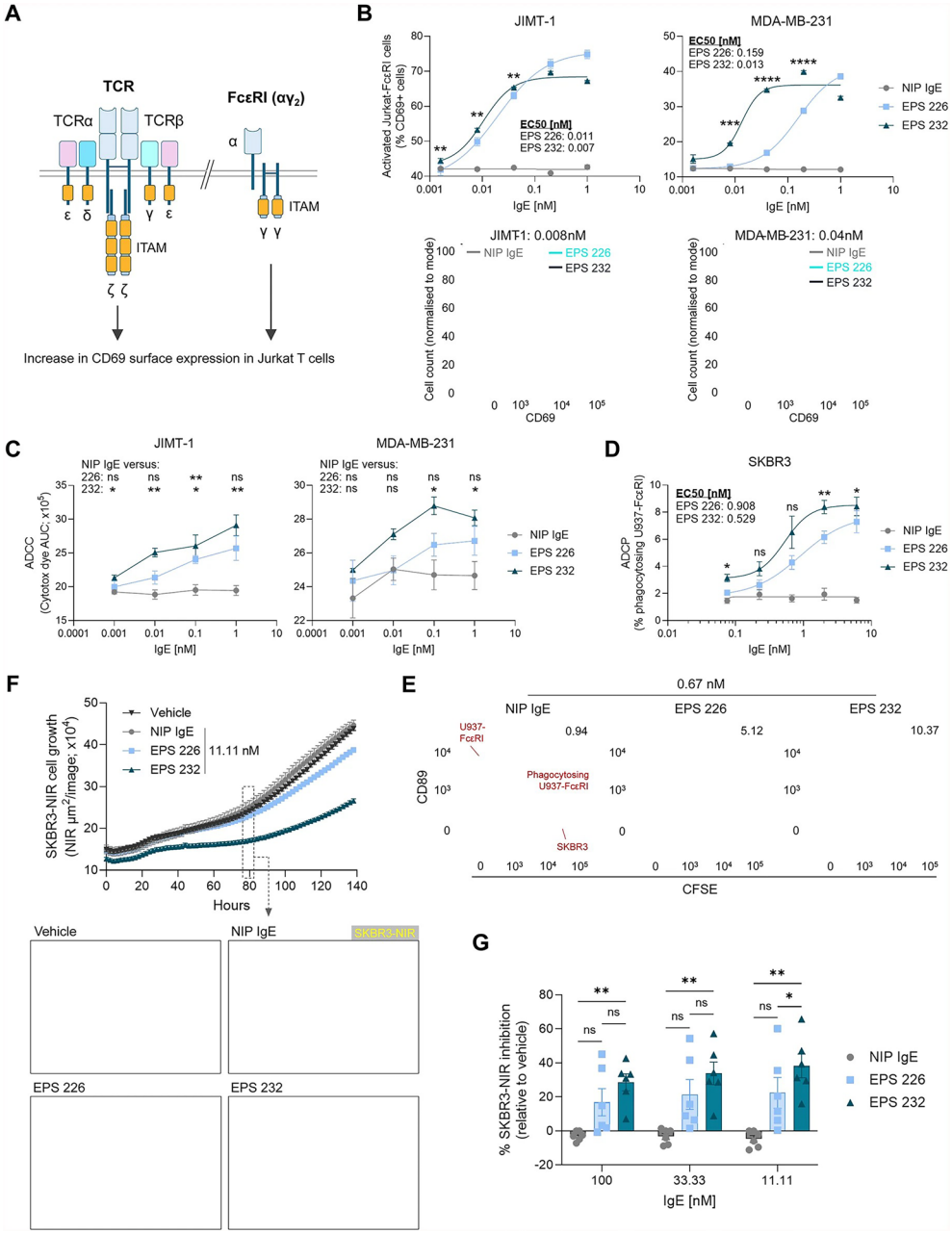
A
TCR
TCRα
TCRβ
FcεRI (αγ2)
α
ε δ γ ε
ITAM
γ γ
ITAM
ζ ζ
Increase in CD69 surface expression in Jurkat T cells
B
JIMT-1
MDA-MB-231
Activated Jurkat-FcεRI cells (% CD69+ cells)
EC50 [nM]
EPS 226: 0.011
EPS 232: 0.007
EC50 [nM]
EPS 226: 0.159
EPS 232: 0.013
IgE [nM]
NIP IgE
EPS 226
EPS 232
JIMT1: 0.008nM
MDA-MB-231: 0.04nM
Cell count (normalised to mode)
CD69
C
JIMT-1
MDA-MB-231
NIP IgE versus:
226: ns ns ** ns
232: * ** * **
ADCC (Cytotox dye AUC; x10^5)
IgE [nM]
NIP IgE
EPS 226
EPS 232
D
SKBR3
EC50 [nM]
EPS 226: 0.908
EPS 232: 0.529
ADCP (% phagocytosing U937-FcεRI)
IgE [nM]
F
Vehicle
NIP IgE
EPS 226
EPS 232
11.11 nM
SKBR3-NIR cell growth (NIR µm²/image; x10⁴)
Hours
Vehicle
NIP IgE
SKBR3-NIR
EPS 226
EPS 232
E
0.67 nM
NIP IgE
EPS 226
EPS 232
U937-FcεRI
0.94
5.12
10.37
Phagocytosing U937-FcεRI
SKBR3
CD89
CFSE
G
% SKBR3-NIR inhibition (relative to vehicle)
IgE [nM]
100
33.33
11.11
NIP IgE
EPS 226
EPS 232

◀**Fig. 2**. EPS 232 is more potent and efficacious than EPS 226. (**A**) Cartoon comparing the structures of the T cell receptor (TCR) and the FcεRI($\alpha\gamma_2$) receptor, which both possess intracellular ITAMs. (**B**) Jurkat-FcεRI($\alpha\gamma_2$) cells were cultured at a 1:1 E:T with target JIMT-1 cells (left) or MDA-MB-231 cells (right) with either NIP IgE, EPS 226 or EPS 232 for 18 h. Activation of Jurkat-FcεRI cells was measured by expression of CD69. Top: data points show mean, error bars are SEM, n = 6, two independent experiments. Two-way ANOVA comparing EPS 226 to EPS 232, Tukey's multiple comparisons test. Bottom: representative flow cytometry plots of CD69 expression in Jurkat-FcεRI cells upon culture with JIMT-1 (left; 0.008 nM IgE) or MDA-MB-231 (right; 0.04 nM IgE) cells. (**C**) RBL-SX38 cells were cultured with either NIP IgE, EPS 226 or EPS 232 in the presence of JIMT-1 (left) or MDA-MB-231 (right) cells (6:1 E:T) for 44 h. Cytotoxicity was measured on the Incucyte® SX5. Data points show mean average, error bars are SEM, n = 4, two independent experiments. Two-way ANOVA comparing to NIP IgE, Dunnett's multiple comparisons test. (**D**) U937-FcεRI($\alpha\gamma_2$) cells were cultured with CFSE-labelled target SKBR3 cells (2:1 E:T) with either NIP IgE, EPS 226 or EPS 232 for 24 h, where ADCP was assessed by flow cytometry by measuring for CFSE + U937-FcεRI cells. Data points show mean average, error bars are SEM, n = 6 from three independent experiments. (**E**) Representative ADCP flow cytometry plots from the experiment described in (**D**) at 0.67 nM IgE treatment. (**F**) Primary monocyte-derived macrophages were cultured with vehicle, NIP IgE, EPS 226 or EPS 232 (11.11 nM) in the presence of SKBR3-NIR cells (8:1 E:T) for six days. Top: Representative graph from one of six donors tested, n = 3 per condition, mean average being shown, error bars are SEM. Bottom: representative image from Incucyte® analysis at 78 h treatment with SKBR3-NIR cells shown in yellow. (**G**) Mean average SKBR3-NIR cell growth inhibition relative to vehicle treatment from experiment described in (**F**). Each data point is a different biological donor (n = 6). Error bars represent SEM. Two-way ANOVA, Tukey's multiple comparisons test.

Fig. 3. EPS 232 maintains same HER2 epitope as EPS 226. The three-dimensional structure of the HER2-EPS 232 Fab complex is shown in surface representation (**A**) and cartoon representation (**B**). In both views, the variable domains of the heavy chain and light chain are coloured in wheat and raspberry, respectively. HER2 domain I (DI) is coloured in deep teal (residues 23–217), domain II (DII) in sky blue (218–314), and domain III (DIII) in green (342–500). (**C**) Superposition of both HER2-Fab complexes, displayed in cartoon representation, with HER2-EPS 226 in green and HER2-EPS 232 in blue. (**D**) Intermolecular interactions between EPS 232 CDR loops and HER2 are shown in stick form, with the surrounding backbone in ribbon form. On the left panel, LCDR1 is shown in hot pink, LCDR2 in grey and LCDR3 in lime, with HER2 shown in sky blue. Mutated residues (Thr 52 and Ser 98) present in the light chain, which do not directly contribute to the binding interface, are shown by a red arrow. On the right panel, HCDR1 is shown in hot pink, HCDR2 in grey and HCDR3 in lime, with HER2 shown in sky blue. (**E**) Residues from heavy and light chain CDR loops 1, 2 and 3 that contact HER2 are shown as a sequence alignment. The same colour scheme is maintained as in (**D**), and only residues making contact are coloured and underlined. The residue at the start of the CDR loop is numbered. For emphasis, mutated residues Glu/Thr 52 and Thr/Ser 98 are shown in a bigger font in the alignment. (**F**) HER2 residues from domain II, starting from residue 266, that contact the Fabs are coloured blue and underlined in a sequence alignment.

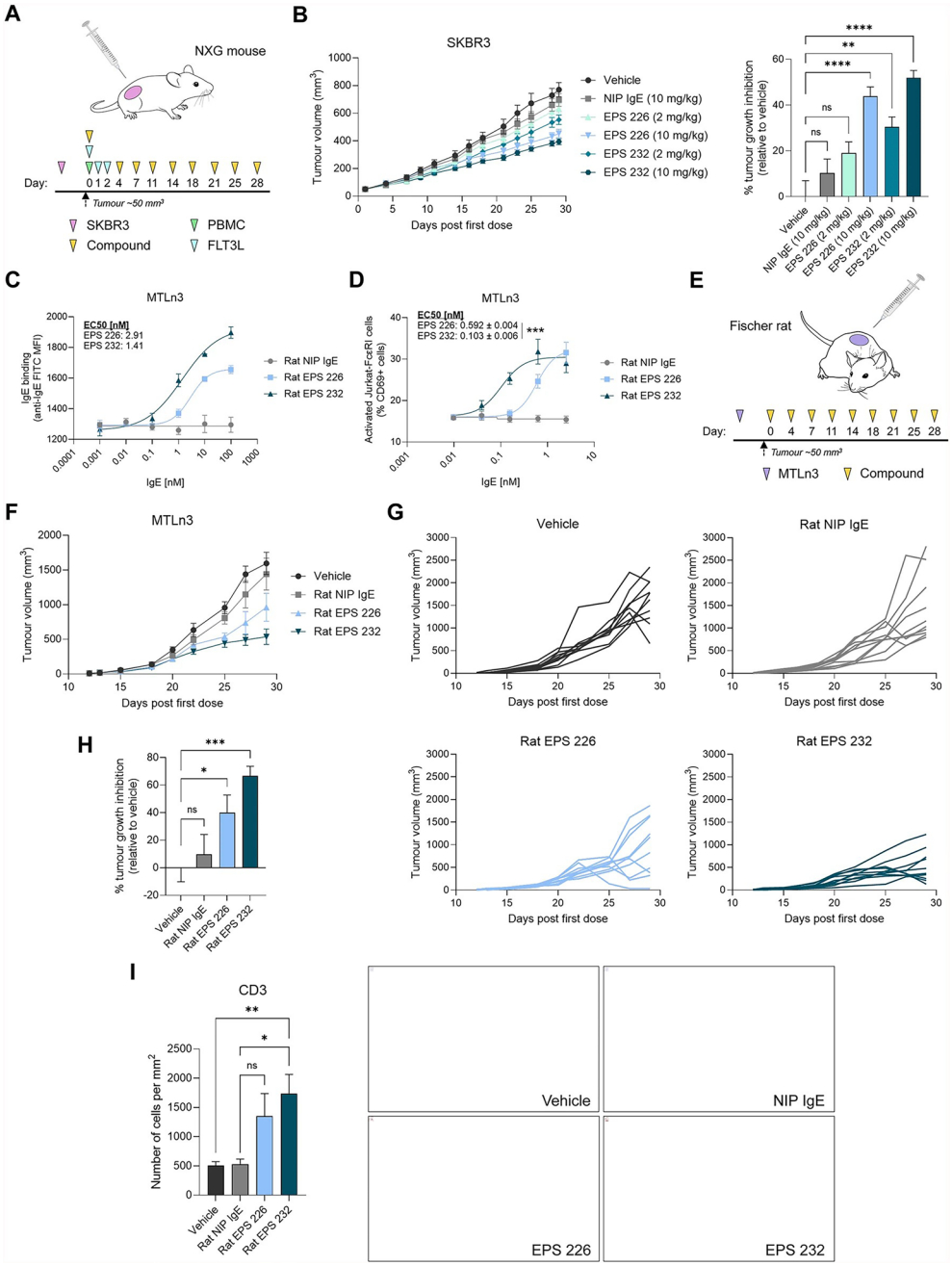

Fig. 4. EPS 232 induces greater anti-tumour activity compared to EPS 226. (**A**) NXG mice subcutaneously implanted with 1×10^7 SKBR3 cells were intravenously treated with vehicle, NIP IgE (10 mg/kg), EPS 226 or EPS 232 (2 or 10 mg/kg), alongside 5×10^6 human PBMCs. Mice were dosed with the compounds twice weekly. (**B**) Left: tumour growths from experiment described in (**A**). 12 mice per group, three PBMC donors. Data points show mean, error bars are SEM. Right: tumour growth inhibition (TGI) at day 29 relative to vehicle. Bars show mean TGI, error bars are SEM, one-way ANOVA, Tukey's multiple comparisons test relative to NIP IgE. (**C**) MTLn3 cells were treated with rat NIP IgE, rat EPS 226 or rat EPS 232; where bound IgE was detected using an anti-IgE FITC conjugated antibody. Data points show mean, error bars are SEM, n = 6, two independent experiments. (**D**) Jurkat-FcεRI($\alpha\gamma_2$) cells were cultured with MTLn3 cells (1:1 E:T) with rat NIP IgE, rat EPS 226 or rat EPS 232 for 18 h, where cells were stained for CD69. Bars show mean, error bars are SEM, n = 6, three experiments, paired t-test of EC50s (n = 3). (**E**) Fischer rats subcutaneously implanted with 7×10^5 MTLn3 cells were dosed with vehicle, rat NIP IgE, rat EPS 226 or rat EPS 232 (10 mg/kg) subcutaneously twice weekly. (**F**) Tumour growths from experiment described in (**E**), 10 rats per group, data points show mean, error bars are SEM. (**G**) Individual rat MTLn3 growth curves from data shown in (**F**). (**H**) TGI at day 29 relative to vehicle from the experiment described in (**E**). Bars show mean TGI, error bars are SEM. One-way ANOVA, Dunnett's multiple comparisons test relative to NIP IgE. (**I**) Tumours from the experiment described in (**E**) were excised at the end of study and stained for CD3 by immunohistochemistry. Left: Bars show mean of CD3 + cells present, error bars are SEM. One-way ANOVA, Tukey's multiple comparisons test. Right: Representative images of CD3 + cells within the tumour. Bar represents 100 µm.